Electronic Supplementary Information_1 (ESI_1)

for

Carbon and nitrogen-based gas fluxes in subarctic ecosystems under climate warming and increased cloudiness

Flobert A. Ndah[*], Marja Maljanen, Riikka Rinnan, Hem Raj Bhattarai, Cleo L. Davie-Martin, Santtu Mikkonen, Anders Michelsen, Minna Kivimäenpää

[*]Corresponding author: Flobert A. Ndah, Department of Environmental and Biological Sciences, University of Eastern Finland, P.O Box 1627, 70211, Kuopio, Finland. Email: flobert.ndah@uef.fi

Gas flux measurements, analyses, and calculations

CH_4 and N_2O fluxes were measured using a static chamber system (Fig. S1). PVC chambers (V = 4.8 l) were inserted over soil cores and 25 ml gas samples were taken from the chamber headspace with a 60 ml syringe at intervals of 5, 15, 25 and 35 minutes after enclosure. Gas samples (25 ml) were injected immediately into 12 ml evacuated vials (Labco Exetainers®, UK). The concentration of gas samples was analysed with a gas chromatograph (Agilent 7890B, Agilent Technologies, USA) equipped with an autosampler (Gilson GX – 271, Gilson Inc, USA). The flux rates were calculated from the linear change (increase or decrease) in the gas concentrations in the chamber headspace.

HONO and NO fluxes were measured by establishing a dynamic chamber system (Fig. S2).[1] Measurements were conducted in a dark room with a temperature of +21°C. The dynamic chamber system setup consisted of a 3.2L Teflon chamber, which was connected to a commercial long path absorption photometer (LOPAP) HONO analyzer (QUMA Elektronik & Analytik GmbH, Germany) for HONO and a Thermo 42i NOx analyzer (Thermo Fisher Scientific, USA) for NO allowing simultaneous measurement of HONO and NO. At the top of the chamber were four Teflon tubes (ID: 4 mm); an inlet tube used to flush the headspace purified air at a rate of 4 Lmin^{-1}, two outlet tubes carrying the sample air from the chamber headspace to the LOPAP and NOx analyzers (one connects the soil core with the external sampling unit of LOPAP and the other with the NOx analyzer), and an additional outlet tube that flushes excess air from the system (length = 88 cm). The length of the outlet tube connected to the LOPAP was 44 cm and that connected to the NOx analyzer was 176 cm.

For HONO, sample measurements were terminated after getting a stable plateau in channel 1 which took approx. 1 - 1.5 hour. Prior to connecting any samples with LOPAP, the chamber headspace was flushed for ten minutes with purified air i.e., pressurized air filtered through active carbon and Purafil Select Media® pellets and a high-efficiency particulate arrestance (HEPA) filter to remove any VOC, NOx and SO_2 impurities and particles, and have relative humidity of ~ 8 %. This ensured that the headspace was free from ambient HONO. In the meantime, LOPAP was run under zero air (synthetic air of purity 5.0; 79 % N_2 and 21 % O_2) to see any possible base line shift of the instrument. At least two zero air runs of 50 minutes and two empty PVC cores with Teflon chamber on top (bottom sealed with Al folio) for again 50 minutes were measured on the day of every HONO and NO measurement. Zero air measurements between samples allowed for the determination of any change in LOPAP sensitivity, while the measurement of blank samples (empty PVC cores) provided information on the background HONO [via heterogeneous process like NO_2 hydrolysis[2]] and NO emissions from the whole system be it soil core, chamber and tubes inner surfaces, or purified air. The LOPAP was operated at 10 % of relative error and with the detection limit (DL) of ca. 3-5.3 ppt over the whole

experimental period. NO was measured at a flow rate of 0.700 L min-1 with a DL of 0.4 ± 0.2 ppb. On every measurement occasion, the lab air concentration of HONO and NO was always checked and ensured to be below or closer to the DL of the LOPAP and NOx analyzers, respectively. Calibration of LOPAP was performed as described by Bhattarrai et al[1]. The summary of the parameters of LOPAP used during the measurements are similar to those used by Bhattarrai et al[1] but for the gas flow rate and response time (time taken by the device to rise to 90 % of full the signal) which were 1 L min^{-1} and 4.36 minutes, respectively. HONO and NO measurements were done for a period of one hour per sample. For NO, six data points every minute (one data point/10 sec) were recorded in real time by a computer connected to the NOx analyzer device.

HONO, NO, CH$_4$ and N$_2$O flux calculations

The real HONO concentrations (ppt) from the samples were calculated as described by Bhattarrai et al[1]. HONO, NO, CH$_4$ and N$_2$O fluxes were calculated using the following equations (1 & 2) from Bhattarrai et al[1]. HONO and NO fluxes were calculated using equation (1) while the flux rates of CH$_4$ and N$_2$O were calculated based on linear change (increase or decrease) in the gas concentrations in the chamber headspace using equation (2).

$$F = \frac{f_v}{1000} * \frac{1}{V_m} * \frac{T_0}{(T_0 + T)K} * \frac{p}{p_0} * \frac{\Delta c}{10^9} * \frac{60 * h * M}{A} * 10^6 \qquad (1)$$

$$F = \frac{p_0 * k * V * M}{R * T * A} * 60 \qquad (2)$$

Where F = flux rate (μg CH$_4$-C m^{-2} h^{-1} for CH$_4$ and μg N m^{-2} h^{-1} for N$_2$O, NO, and HONO), f$_v$ = flow rate (cm^3 min^{-1}), V$_m$ = 22.4136 l mol^{-1}, T$_o$ = 273.15K, T = chamber temperature (K), p = air pressure (kPa), p$_0$ = 101.3 kPa, ΔC = concentration difference (ppb). k = CH$_4$ or N$_2$O slope (ppm h^{-1}), V = volume of the chamber headspace (m^3), R = ideal gas constant (8.314 J k^{-1} mol^{-1}), M = molar mass (g mol^{-1}) of respective gas, A = sample/collar area (m^2).

BVOCs were measured using a dynamic enclosure technique (Fig. S3). Precleaned (120° C, 1 h) transparent polyethylene terephthalate (PET) bags (45 × 55 cm, Rainbow, Finland) were used as enclosures.[3] The opening of the PET bag was tied around the mesocosm enclosing the entire mesocosm area, containing plants and soil, to ensure BVOC sampling at ecosystem-level. Water filled on aluminum plates under each mesocosm ensured the system was kept air-tight during sampling. Air was circulated through the PET bags using battery-operated pumps (12 V; Rietschle Thomas,

Puchheim, Germany). The air inlet was led through a cut corner in the PET bag secured with a wire and the system flushed for 15 min before the measurement with an inflow rate of 600 ml min^{-1}. Subsequently, the adsorbent cartridge was inserted via another cut corner into the PET bag secured with a wire. During the 60-min sampling period, air was circulated through the enclosure with an inflow rate of 600 ml min^{-1} and an outflow rate of 200 ml min^{-1}. The flow rates were calibrated using a mini–BUCK Calibrator (A.P. Buck, Inc. Orlando, Florida, USA). The incoming air was filtered for particles and background hydrocarbons and scrubbed for ozone in order to avoid losses of the highly reactive BVOCs.[4] BVOCs from the 6 L air sample were adsorbed in stainless steel cartridges (Markes International Ltd., Llantrisant, UK) containing Tenax TA (125 mg) and Carbopack B (125 mg). After sampling, the cartridges were sealed with Teflon-coated brass caps and stored at + 4°C until analysis. Blank sampling was conducted to account for compounds derived from sampling materials and the analytical system. Blank sampling was achieved by sinking empty (without plants or soil) mesocosm/PVC cores in water and the PET bag was tied around the cores such that upper edges of the cores were included in the sampling. The water level corresponded to the average height of soil surface in the mesocosms. A new PET bag was used for each measurement.

BVOC samples were analyzed using gas chromatography–mass spectrometry (Hewlett-Packard GC type 6890, Germany; MSD 5973, UK) after thermal desorption with automatic thermal desorber (Perkin-Elmer ATD400 Automatic Thermal Desorption system, Wellesley, MA, USA) at 250 °C for 10 min and cryofocusing at −30 °C. The carrier gas was helium with a constant flow rate of 1.2 mL min^{-1}. The oven temperature was held at 40 °C for 2 min and then programmed to ramp to 210 °C at a rate of 5 °C min^{-1} and finally to 250 °C at a rate of 20 °C min^{-1}. An HP-5MS capillary column (model 19091S-436; 60 m × 0.25 mm i.d (inner diameter) × 0.25 μm film thickness; Agilent, Santa Clara, CA, USA) was used for the separation of BVOCs. Chromatograms were analyzed using the software PARADISe v. 3.8.[5] Compounds were identified using pure standards, when available, or tentatively identified using the NIST 2014 Mass Spectral Library (National Institute of Standards and Technology, Gaithersburg, MD, USA). For tentative identification, only compounds with a match factor >800 and probability >30 were considered for further analysis. BVOC concentrations were quantified using external standards. Compounds for which pure standards were unavailable were quantified using the closest structurally related standard compound (Table S1). Compounds that are known to arise from plastics, the analytical system, sorbent tubes, or personal care products were excluded from the dataset, including siloxanes, phthalates, dibutyl adipate, 2-ethylhexyl salicylate, and homosalate. Compounds smaller than isoprene were also excluded from the dataset because the adsorbent cartridges cannot reliably trap lighter VOCs. VOC concentrations in blanks were subtracted

from those in the samples. VOC concentrations and emission rates were calculated for every compound using the equations:

VOC concentration (ng l^{-1}) = *(mass of VOC in sample (ng) – average mass of VOC in blank (ng))/ (sampling time of 60 (min) × air flow rate through the cartridge 0.2 (l min^{-1}))*

VOC emission (ng VOC m^{-2} ground area hour^{-1}) = *(VOC concentration (ng l^{-1}) × (air flow rate into the chamber 0.6 (l min^{-1}) × 60 (min)))/surface area of collar (m^2)*

Fig. S1 CH_4 and N_2O measurement set up in the laboratory using static dark chamber method. The chamber is positioned over the soil core and gas sampled from the chamber headspace with syringe into evacuated vials.
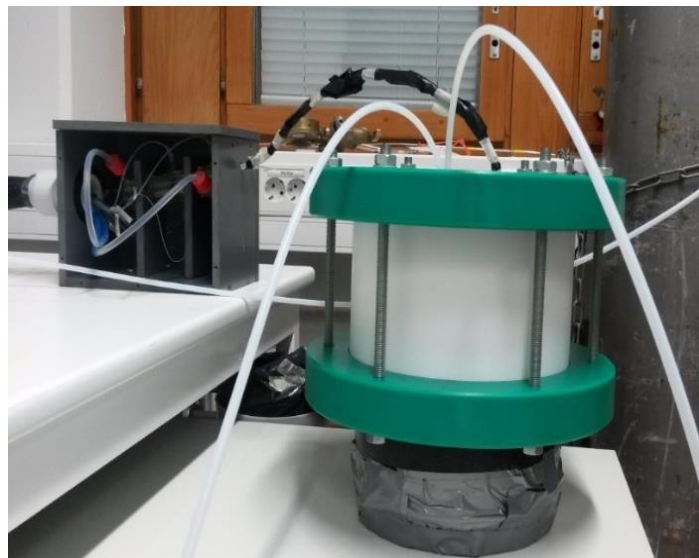
Fig. S2 HONO measurement set up in the laboratory - a Teflon chamber is positioned over the soil core and connected to the LOPAP via the external sampling unit for HONO analysis and NOx analyzer for NO (Bhattarai et al[1]).
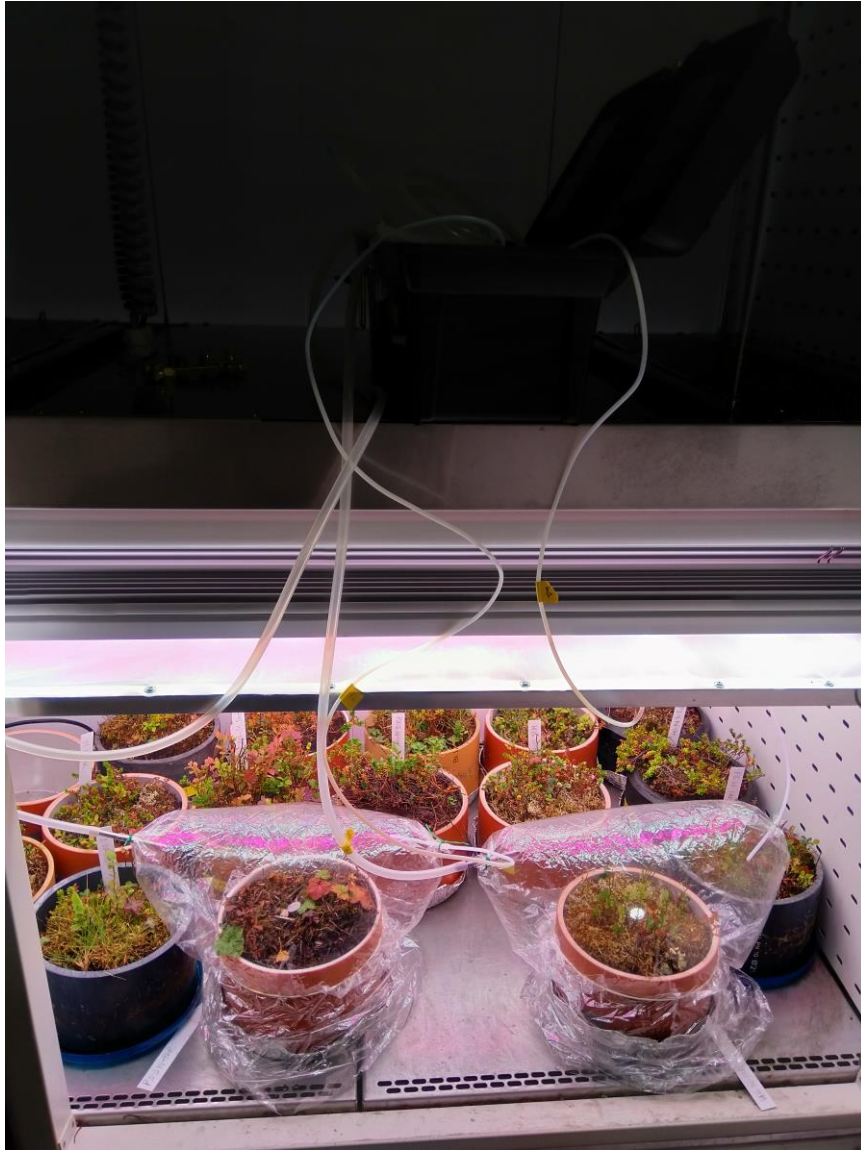
Fig. S3 BVOC measurement set up in the laboratory using dynamic enclosure technique.

Table S1 Standard assignment for tentatively identified compounds without their own standard.

Tentatively identified compounds			Standard assignment
Compound group	**Compound class**	**Specifics**	
hydrocarbons	alkane	C6	hexane
		C7	toluene
		C8	octane
		C9	nonane
		<C12	hexane
		Cyclic or ≥C12	camphene
	alkene	≤C5	isoprene
		C6-C10	toluene
		≥C10	ocimene
		cyclic	camphene
	benzenoids	all	toluene
isoprene	isoprene	C5H8	isoprene
monoterpenes	non-oxygenated monoterpenes	no O	α-pinene
	oxygenated monoterpenes	≥ 1 O	eucalyptol
sesquiterpenes	non-oxygenated sesquiterpenes	no O	humulene
	oxygenated sesquiterpenes	≥ 1 O	caryophyllene oxide
oxygenated VOCs	acid (=O, OH)	<C9	cis-3-hexenyl acetate
		≥C9	cis-3-hexenyl butyrate
	alcohol (-OH)	<C8	cis-3-hexen-1-ol
		≥C8	1-octen-3-ol
	aldehyde (=O, -H)	<C8, no C=C	hexanal
		<C8, with C=C	trans-2-hexen-1-al
		C8	nonanal
		>C8	nonanal
	ester (=O, -OR)	<C9	cis-3-hexenyl acetate
		≥C9	cis-3-hexenyl butyrate
		cyclic/ ≥ 3 O	methyl salicylate
	furan	only 1 O	cis-3-hexenyl butyrate
		> 1 O	methyl salicylate
	ketone (=O)	<C8	4-methyl-2-pentanone
		C8	nonanal
		>C8	nonanal
	oxygenated benzenoids	only 1 O	cis-3-hexenyl acetate
		> 1 O	methyl salicylate
	other oxygenated VOCs	<C9	cis-3-hexenyl acetate
		≥C9	cis-3-hexenyl butyrate
		cyclic/ ≥ 3 O	methyl salicylate
other VOCs	halogens (-Cl, -Br, -F)	all	toluene
	nitrogen-containing VOCs	all	toluene
	other	all	toluene
	sulphur-containing VOCs	all	toluene

Table S2 Compounds present in an HC-48 Component Indoor Air Standard used for tentatively identified compounds.

Compounds
hexane
2,4-dimethylpentane
benzene
4-methyl-2-pentanone
n-octane
toluene
n-nonane
ethylbenzene
m-xylene
p-xylene
o-xylene
styrene
n-decane
1,3,5-trimethylbenzene
n-undecane
n-dodecane
n-tridecane
n-tetradecane
n-pentadecane
n-hexadecane

Table S3 Simple main effect (SME) test results for the gas flux variables in the first growing season. Abbreviations: S = site, W × S = warming × site, W × T = warming × time, W × -PAR × T = warming × increased cloudiness × time, W × S × T = warming × site × time, -PAR × S × T = increased cloudiness × site × time, W × -PAR × S × T = warming × increased cloudiness × site × time. W+ = warming treatments (i.e. warming alone and warming + increased cloudiness), W- = treatments without warming (i.e. control and increased cloudiness alone), -PAR+ = increased cloudiness treatments (i.e. increased cloudiness alone and warming + increased cloudiness), -PAR- = treatments without increased cloudiness (i.e. control and warming alone treatments), T1 and T2 indicate the two locations within the tundra, and P indicates the palsa mire. ↓ indicates a decreasing effect and ↑ indicates an increasing effect of the tested factor. For CH_4 flux (CH_4 uptake), ↓ indicates an increasing effect (i.e. increased uptake) and ↑ indicates decreasing effect (i.e. decreased uptake) of the tested factor. Only statistically significant P-values < 0.05 are shown. See text below (*) and appendix A of the article for detailed explanation/interpretation of statistical terms. Statistical terms used as example explanations are highlighted in colour.

Tested variable	Main/Interaction effects	SME comparison	SME test P-value	change
Methane (CH_4)	W × -PAR × S × T	W+ vs W- in -PAR-, P site and early July	< 0.001	↓ -2250 %
		W+ vs W- in -PAR-, P site and mid-July	< 0.001	↓ -750 %
		W+ vs W- in -PAR-, P site and late July	< 0.001	↓ -1700 %
		W+ vs W- in -PAR-, P site and late August	0.025	↓ -100 %
		W+ vs W- in -PAR-, T2 site and early July	0.030	↓ -375 %
		-PAR+ vs -PAR- in W+, P site and mid-June	0.011	↑ 78.3 %
		-PAR+ vs -PAR- in W+, P site and early July	< 0.001	↑ 91.5 %
		-PAR+ vs -PAR- in W+, P site and mid-July	0.002	↑ 82.4 %
		-PAR+ vs -PAR- in W+, P site and late July	< 0.001	↑ 83.3 %
		-PAR+ vs -PAR- in W+, P site and late August	0.022	↑ 101.1 %
		-PAR+ vs -PAR- in W+, T2 site and early July	0.017	↑ 84.2 %
Ecosystem respiration (ER)	S	T1 vs P site	0.018	
		T2 vs P site	0.018	
Gross ecosystem production (GEP)	S	T1 vs P site	0.042	
		T2 vs P site	0.040	
Net ecosystem exchange (NEE)	W × S	W+ vs W- in P site	0.002	
Oxygenated monoterpenes (oMT)	W × T	W+ vs W- in mid-June	0.043	↓ -35.7 %
		W+ vs W- in early July	0.002	↑ 184.0 %
		W+ vs W- in mid-July	< 0.001	↑ 258.8 %
		W+ vs W- in mid-August	0.002	↑ 116.2 %
		W+ vs W- in late August	0.012	↑ 129.4 %
	-PAR × S × T	-PAR+ vs -PAR- in T2 site and mid-June	0.005	↓ -70.6 %
		-PAR+ vs -PAR- in P site and mid-June	0.003	↓ -62.6 %
		-PAR+ vs -PAR- in P site and mid-July	0.044	↓ -63.7 %
		-PAR+ vs -PAR- in T1 site and mid-July	< 0.001	↓ -63.1 %
		-PAR+ vs -PAR- in T1 site and late August	0.026	↓ -63.7 %
Sesquiterpenes (SQT)	W × S × T	W+ vs W- in T1 site and early July	0.002	↑ 21.2 %
		W+ vs W- in T1 site and mid-July	0.004	↑ 17.3 %
		W+ vs W- in T1 site and mid-August	<0.001	↑ 27.2 %
		W+ vs W- in T1 site and late August	0.028	↑ 15.6 %
		W+ vs W- in P site and early July	0.025	↑ 15.7 %
		W+ vs W- in P site and mid-July	0.040	↑ 12.6 %
		W+ vs W- in P site and late August	0.033	↑ 16.3 %
		W+ vs W- in T2 site and early July	0.006	↑ 18.6 %
Oxygenated VOCs (OVOC)	-PAR × S × T	-PAR+ vs -PAR- in T2 site and mid-June	< 0.001	↓ -66.3 %
		-PAR+ vs -PAR- in P site and mid-June	< 0.001	↓ -70.2 %
		-PAR+ vs -PAR- in P site and mid-July	0.023	↓ -50.7 %
		-PAR+ vs -PAR- in T1 site and late-July	0.030	↑ 123.0 %
	W × -PAR × T	W+ vs W- in -PAR+ and mid-June	0.015	↓ -77.2 %
		-PAR+ vs -PAR- in W+ and mid-June	< 0.001	↓ -82.6 %
		-PAR+ vs -PAR- in W+ and early July	0.039	↓ -45.3 %
		-PAR+ vs -PAR- in W+ and mid-July	< 0.001	↓ -51.8 %

(Continued on next page)

(continued)

Tested variable	Main/Interaction effects	SME comparison	SME test *P*-value	change
Oxygenated Sesquiterpenes (oSQT)	-PAR × S × T	-PAR+ vs -PAR-, P site and mid-June	< 0.001	↑ 292.4 %
		-PAR+ vs -PAR-, T2 site and early July	0.015	↓ -96.6 %
Other VOCs	-PAR × S × T	-PAR+ vs -PAR- in P site and mid-June	0.001	↓ -71.9 %
		-PAR+ vs -PAR- in P site and late August	0.009	↑ 409.2 %
		-PAR+ vs -PAR- in T2 site and mid-June	0.002	↓ -75.0 %
		-PAR+ vs -PAR- in T1 site and mid-July	0.008	↓ -36.2 %
Monoterpenes (MT)	W × -PAR × T	W+ vs W- in -PAR+ and early July	0.029	↓ -44.0 %
		-PAR+ vs -PAR- in W+ and mid-June	< 0.001	↓ -69.5 %
		-PAR+ vs -PAR- in W+ and mid-July	0.004	↓ -61.3 %
Hydrocarbons (HC)	W × -PAR × T	W+ vs W- in -PAR+ and mid-June	<0.001	↓ -82.0 %
		W+ vs W- in -PAR+ and early July	0.007	↑ 1233.0 %
		W+ vs W- in -PAR+ and late August	0.023	↑ 118.8 %
		-PAR+ vs -PAR- in W+ and mid-July	0.012	↓ -63.5 %
		-PAR+ vs -PAR- in W+ and late July	0.009	↑ 302.6 %
		-PAR+ vs -PAR- in W+ and mid-August	0.006	↑ 786.2 %
		-PAR+ vs -PAR- in W+ and late August	0.016	↑ 137.6 %

* Example explanations of simple main effects (SME) comparison statistical terms.

Example 1 (highlighted in light orange, table S3) show that the warming (W+) treatment increased CH_4 uptake by 375 % compared to treatment without warming (W-) and the effect of warming took place in the cloudiness treatment -PAR-, i.e. under no increased cloudiness, in T2 site and in early July of the first growing season.

Example 2 (highlighted in dark orange, table S3) show that the increased cloudiness (-PAR+) treatment decreased CH_4 uptake by 78.3 % compared to treatment without increased cloudiness (-PAR-) and the effect was dependent on warming, i.e. took place in the warming treatment W+, in P site and in mid-June of the first growing season.

Example 3 (highlighted in light green, table S3) show that the increased cloudiness (-PAR+) treatments decreased oMT emission by 70.6 % compared to treatments without increased cloudiness (-PAR-) in T2 site and in mid-June of the first growing season. (The effect of increased cloudiness was not dependent on warming, thus, taking place in both W+ and W-.)

Example 4 (highlighted in dark green, tables S3) show that the warming (W+) treatments increased SQT emission by 21.2 % compared to treatments without warming (W-) in T1 site and in early July of the first growing season.

Example 5 (highlighted in light grey, table S3) show that the warming (W+) treatment decreased OVOC emission by 77.2 % compared to treatment without warming (W-) and the effect of warming was dependent on increased cloudiness, i.e. took place in the increased cloudiness treatment -PAR+, in mid-June of the first growing season.

Example 6 (highlighted in dark grey, table S3) show that the increased cloudiness (-PAR+) treatment decreased OVOC emission by 82.6 % compared to treatment without increased cloudiness (-PAR-) and the effect of increased cloudiness was dependent on warming, i.e. took place in the warming treatment W+, in mid-June of the first growing season.

Table S4 Simple main effect (SME) test results for gas flux variables in the second growing season. Abbreviations: S = site, W × S = warming × site, W × T = warming × time, -PAR × T = increased cloudiness × time, W × -PAR × T = warming × increased cloudiness × time, W × S × T = warming × site × time, -PAR × S × T = increased cloudiness × site × time. W+ = warming treatments (i.e. warming alone and warming + increased cloudiness), W- = treatments without warming (i.e. control and increased cloudiness alone), -PAR+ = increased cloudiness treatments (i.e. increased cloudiness alone and warming + increased cloudiness), -PAR- = treatments without increased cloudiness (i.e. control and warming alone treatments),T1 and T2 indicate the two locations within the tundra and P indicates the palsa mire. ↓ indicates a decreasing effect and ↑ indicates an increasing effect of the tested factor. For CH_4 flux (CH_4 uptake), ↓ indicates an increasing effect (i.e. increased uptake) and ↑ indicates decreasing effect (i.e. decreased uptake) of the tested factor. Only statistically significant *P*-values < 0.05 are shown. See text below (**) and appendix A of the article for detailed explanation/interpretation of statistical terms. Statistical terms used as example explanations are highlighted in colour.

Tested variable	Main/Interaction effects	SME comparison	SME test *P*-value	change
Methane (CH_4)	S	T1 vs P sites	0.005	
	W × -PAR × S	W+ vs W- in -PAR- and T1 site	0.002	↑ 400 %
		W+ vs W- in -PAR- and P site	0.027	↓ -200 %
		-PAR+ vs -PAR- in W+ and T1 site	0.007	↓ -111.1 %
		-PAR+ vs -PAR- in W+ and P site	< 0.001	↑ 95.8 %
Ecosystem respiration (ER)	S	T1 vs P sites	0.035	
		T2 vs P sites	0.005	
Gross ecosystem production (GEP)	S	T1 vs P sites	0.049	
		T2 vs P sites	0.046	
Net ecosystem exchange (NEE)	W × S	W+ vs W- in P site	0.047	↑ 716.1 %
Oxygenated monoterpenes (oMT)	W × T	W+ vs W- in early July	<0.001	↑ 88.3 %
		W+ vs W- in mid-July	<0.001	↑ 247.0 %
		W+ vs W- in late August	0.001	↑ 392.8 %
Other VOCs	W × T	W+ vs W- in late August	< 0.001	↑ 726.6 %
	-PAR × T	-PAR+ vs -PAR- in W- and late August	0.011	↓ -76.6 %
Sesquiterpenes (SQT)	W × S	W+ vs W- in T1 site	0.018	↑ 16.8 %
		W+ vs W- in P site	<0.001	↑ 31.9 %
		W+ vs W- in T2 site	0.025	↑ 9.2 %
Monoterpenes (MT)	W × S × T	W+ vs W- in T1 site and early July	<0.001	↑ 207.0 %
		W+ vs W- in T1 site and mid-July	0.042	↑ 102.0 %
		W+ vs W- in T1 site and late August	0.003	↑ 841.0 %
		W+ vs W- in P site and mid-July	0.001	↑ 377.0 %
		W+ vs W- in P site and late July	<0.001	↑ 475.0 %
	-PAR × T	-PAR+ vs -PAR- in mid-June	0.003	↓ -53.7 %
		-PAR+ vs -PAR- in mid-July	<0.001	↓ -60.1 %
Isoprene	-PAR × S × T	-PAR+ vs -PAR- in P site and mid-July	0.002	↓ -92.6 %
		-PAR+ vs -PAR- in P site and late July	0.045	↓ -89.1 %
		-PAR+ vs -PAR- in P site and late August	0.010	↓ -87.7 %
Oxygenated Sesquiterpenes (oSQT)	-PAR × S × T	-PAR+ vs -PAR- in T2 site and late July	0.002	↓ -88.5 %
Oxygenated VOCs (OVOC)	W × -PAR × T	W+ vs W- in -PAR+ and early July	<0.001	↑ 386.0 %
		-PAR+ vs -PAR- in W+ and early July	0.033	↑ 123.2 %

**Example explanations of simple main effects (SME) comparison statistical terms.

Example 1 (highlighted in light gold, table S4) show that the warming (W+) treatment increased CH_4 uptake by 200 % compared to treatment without warming (W-) and the effect of warming took place in the cloudiness treatment -PAR- i.e. under no increased cloudiness and in the P site.

Example 2 (highlighted in dark gold, table S4) show that the increased cloudiness (-PAR+) treatment increased CH_4 uptake by 111.1 % compared to treatment without increased cloudiness (-PAR-) and the effect of increased cloudiness took place in the warming treatment W+, i.e. was dependent on warming, and in the T1 site.

Example 3 (highlighted in blue, table S4) show that the warming (W+) treatments increased oMT emission by 88.3 % compared to treatments without warming (W-) in early July of the second growing season.

Example 4 (highlighted in red, table S4) show that the warming (W+) treatments increased SQT emission by 16.8 % compared to treatments without warming (W-) and the effect of warming took place in the T1 site.

Example 5 (highlighted in yellow, table S4) show that the increased cloudiness (-PAR+) treatments decreased MT emission by 53.7 % compared to treatments without increased cloudiness (-PAR-) in mid-June of the second growing season.

Methane (CH_4) flux

Across all sites and treatments of the first growing season, CH_4 flux varied significantly according to measurement campaign with the highest uptake in early July (Fig. S4).
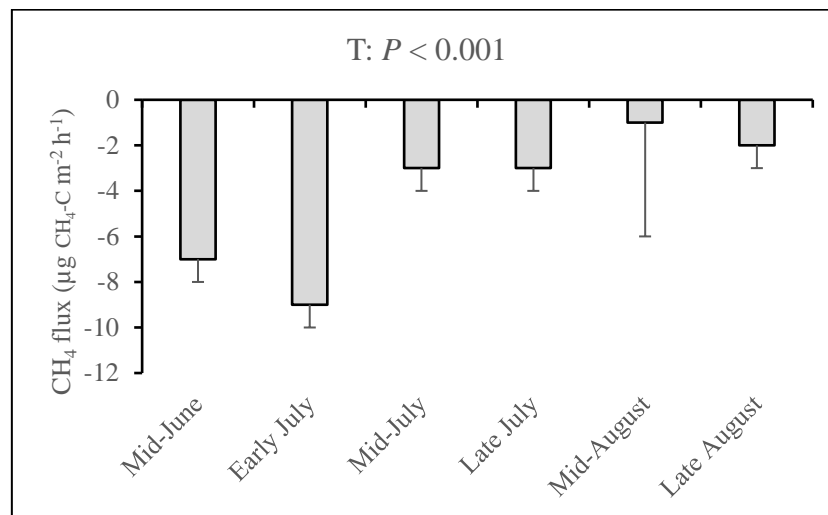
Fig. S4 CH_4 flux from mesocosms across all sites (T1, T2, P) and treatments (control, warming, increased cloudiness, and warming + increased cloudiness) in six measurement campaigns during the first growing season. Bars represent mean values (±SE) measured across all sites and treatments (five replicate mesocosms per site and treatment) per measurement campaign.

A W × -PAR × S × T interaction showed that warming alone increased CH_4 uptake rates for the T2 site in early July, and for the P site in most measurement campaigns (Table S3, Fig. S5). Increased cloudiness had an opposite effect in warming treatments, turning the P site from a net sink to a net source of CH_4 in late August (W × -PAR × S × T interaction, Table S3, Fig. S5).

Across all treatments and measurement campaigns of the second growing season, the T1 site was a source while the T2 and P sites were sinks of CH_4 (Fig. S6) and the T1 and P sites differed significantly (Table S4).
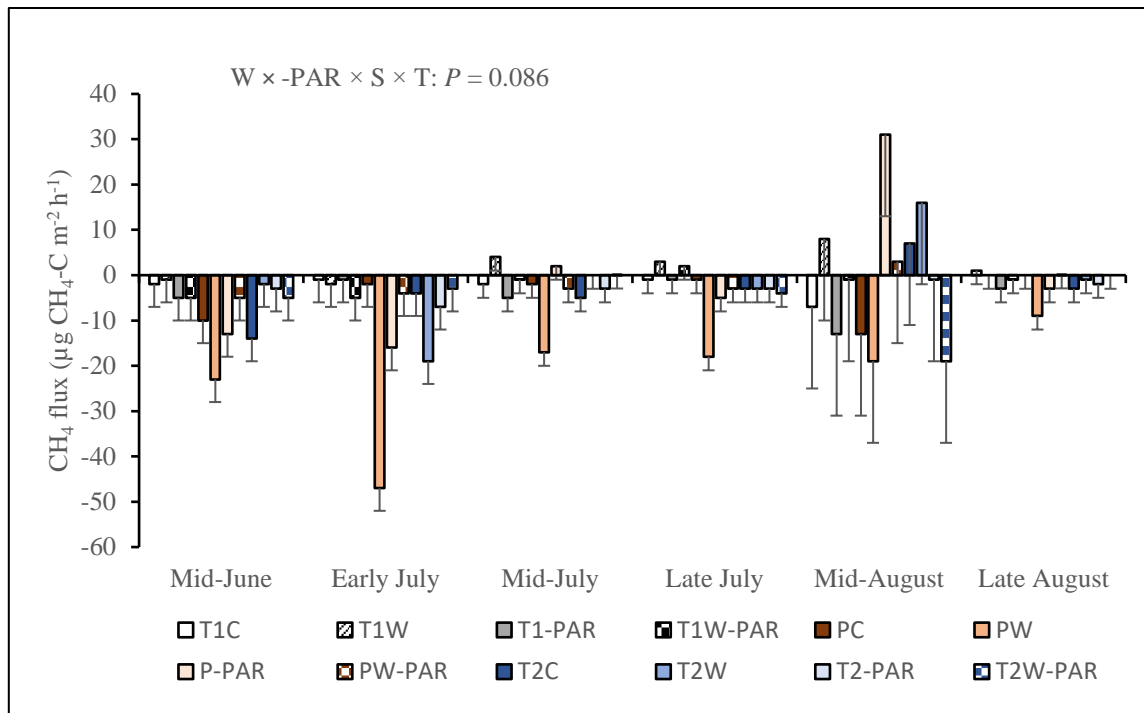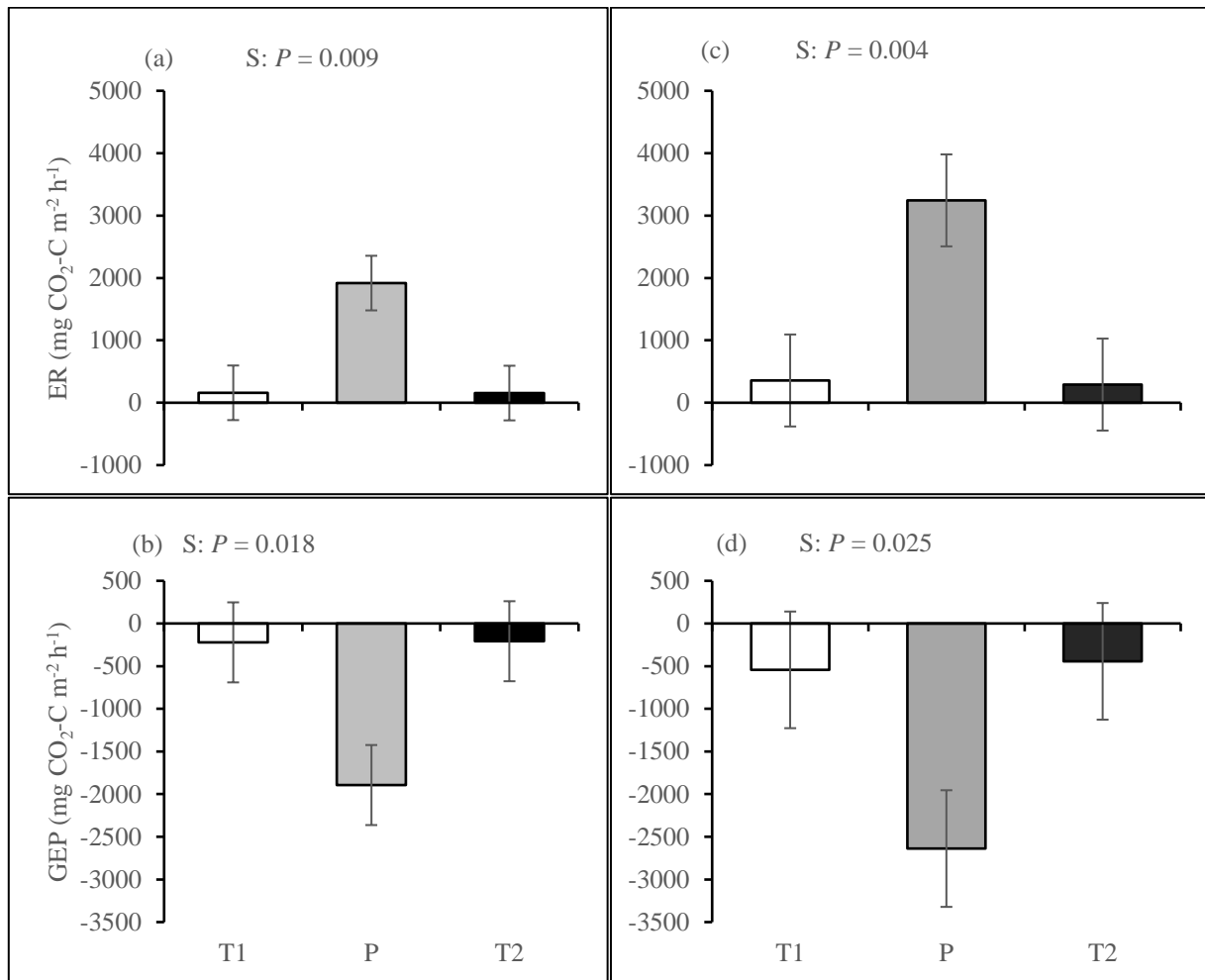
Fig. S5 CH$_4$ fluxes from mesocosms exposed to control (C), warming (W), increased cloudiness (-PAR), and warming + increased cloudiness (W-PAR) treatments during the first growing season. Bars represent mean values per treatment per site (±SE, n = 5 per treatment per site) per measurement campaign. Abbreviations: T1 and T2 indicate the two locations within the tundra, P = palsa mire, T1C = T1 site in control, T1W = T1 site in warming, T1-PAR = T1 site in increased cloudiness, T1W-PAR = T1 site in warming + increased cloudiness, PC = Palsa site in control, PW = Palsa site in warming, P-PAR = Palsa site in increased cloudiness, PW-PAR = Palsa site in warming + increased cloudiness, T2C = T2 site in control, T2W = T2 site in warming, T2-PAR = T2 site in increased cloudiness, T2W-PAR = T2 site in warming + increased cloudiness treatments, W × -PAR × S × T = warming × increased cloudiness × site × time interaction. Marginally significant P-values < 0.1 from LMM ANOVA are shown. See table S3 for detailed statistics.
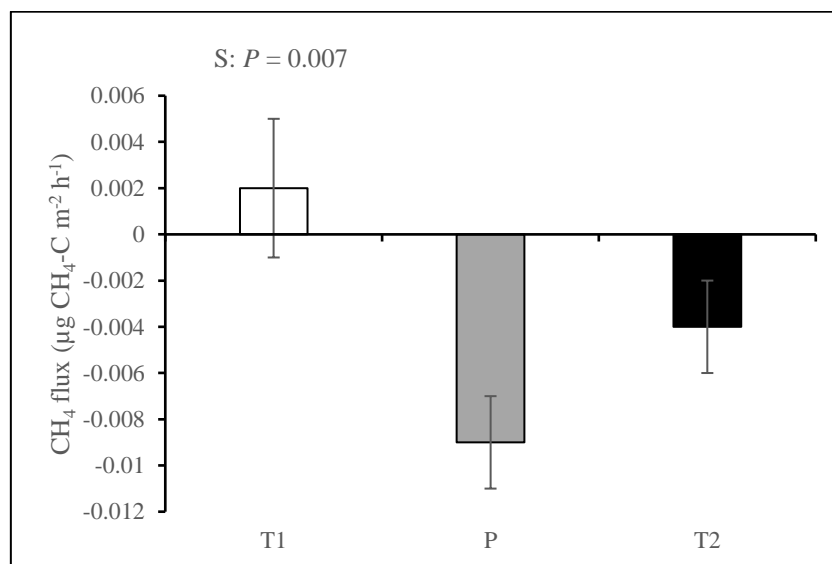
Fig. S6 CH$_4$ flux from mesocosms from T1, T2, and P sites across all treatments (control, warming, increased cloudiness, and warming + increased cloudiness) and measurement campaigns during the second growing season. Bars represent season mean values (±SE, n = 20 per site) across all treatments. Abbreviations: S = site, T = tundra, where T1 and T2 indicate the two locations within the tundra, and P = palsa mire.

Carbon dioxide (CO_2) fluxes

Across all treatments and measurement campaigns in both growing seasons, the P site had a significantly higher ER and GEP than the T1 and T2 sites (Tables S3 & S4, Fig. S7).

Fig. S7 CO_2 fluxes from mesocosms from T1, T2, and P sites exposed to control (C), warming (W), increased cloudiness (-PAR), and warming + increased cloudiness (W-PAR) treatments; Ecosystem respiration (ER) and Gross ecosystem production (GEP) across five measurement campaigns during the first (a,b) and second (c,d) growing seasons. Bars represent season mean values (±SE) measured from mesocosms across all treatments per site (20 replicate mesocosms per site). Abbreviations: S = site, T = tundra, where T1 and T2 indicate the two locations within the tundra, and P = palsa mire. Statistically significant P-values < 0.05 from LMM ANOVA are shown.

BVOC fluxes

Emission profile
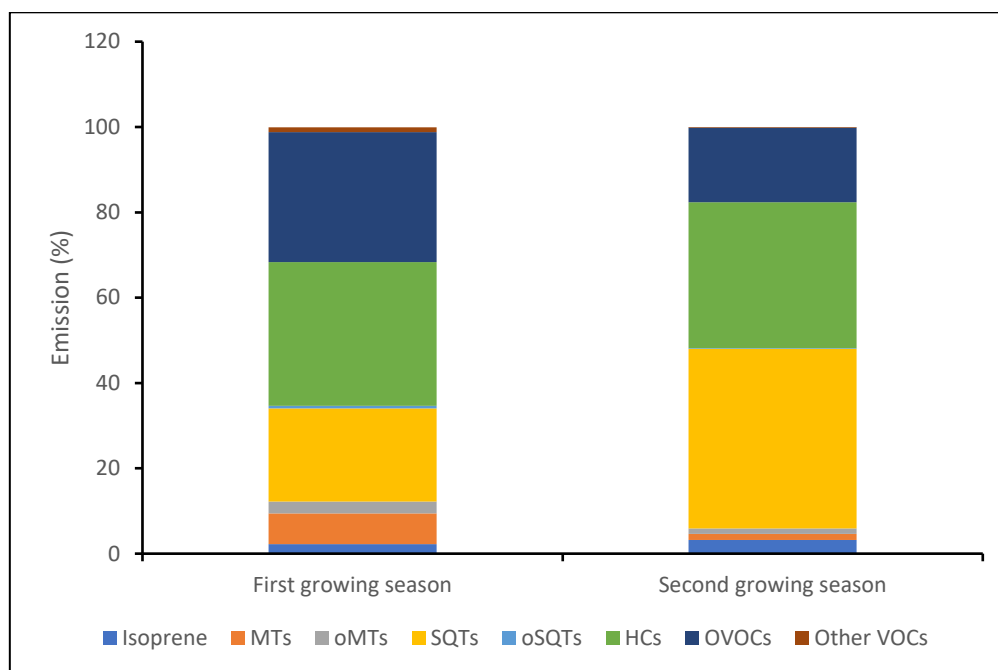
Fig. S8 Percentage contribution of each BVOC group to the total BVOC emissions in both growing seasons. BVOC groups: Isoprene, MTs (monoterpenes), oMTs (oxygenated monoterpenes), SQTs (sesquiterpenes), oSQTs (oxygenated sesquiterpenes), HCs (Hydrocarbons), OVOCs (oxygenated VOCs), and other VOCs.

BVOC responses to warming and or increased cloudiness and interactions with site and or time during the first growing season.

During the first growing season, warming increased SQT emissions in the T1 site in early July, mid-July, mid-August, and late August, in the P site in early July, mid-July, and late August, and in the T2 site in early July (W × S × T interaction, Table S3, Fig. S9). Warming increased oMT emissions across all sites and measurement campaigns except in mid-June where the emissions decreased under warming (W × T interaction, Table S3, Fig. S10) with no significant effects in late July.

Increased cloudiness decreased oMT emissions in the T2 site in mid-June, P site in mid-June and mid-July, and in the T1 site in mid-July and late August (-PAR × S × T interaction, Table S3, Fig. S11a). Other VOC emissions decreased in the T2 and P sites in mid-June, and in the T1 site in mid-July but also increased in the P site in late August (-PAR × S × T interaction, Table S3, Fig. S11b). In response to increased cloudiness, oSQT emissions increased in the P site in mid-June and decreased in the T2 site in early July (-PAR × S × T interaction, Table S3, Fig. S12a). OVOC emissions decreased in response to increased cloudiness in the T2 site in mid-June and in the P site in mid-June and mid-July but increased in the T1 site in late July (-PAR × S × T interaction, Table S3, Fig. S12b).

Warming decreased OVOC emissions in increased cloudiness treatments in mid-June while increased cloudiness had the same effect in warming treatments in mid-June, early July, and mid-July (W × -PAR × T interaction, Table S3, Fig. S13a). Warming decreased MT emissions in increased cloudiness treatments in early July and increased cloudiness had the same effect in warming treatments in mid-June and mid-July (W × -PAR × T interaction, Table S3, Fig. S13b). Warming decreased HC emissions in increased cloudiness treatments in mid-June and increased it in early July and late August while increased cloudiness decreased the emissions in warming treatments in mid-July and increased it in late July, mid-August, and late August (W × -PAR × T interaction, Table S3, Fig. S13c).

BVOC responses to warming and or increased cloudiness and interactions with site and or time during the second growing season.

During the second growing season, warming increased MT emission in the T1 site in early July, mid-July, and late August and in the P site in mid-July and late July (W × S × T interaction, Table S4, Fig. S14). oMT and other VOC emissions also increased in response to warming across all sites, but the effect was significant in early July, and mid-July for oMT, and in late August for oMT and other VOCs (W × T interaction, Table S4, Fig. S15). Across all sites, increased cloudiness decreased the emissions of MT in mid-June and mid-July and other VOC emissions in late August (-PAR × T interaction, Table S4, Fig. S16). Increased cloudiness decreased isoprene emission in the P site in mid-July, late July, and late August and oSQT emissions in the T2 site in late July (-PAR × S × T interaction, Table S4, Fig. S17). Warming and increased cloudiness, in combination with each other, increased OVOC emissions in early July (W × -PAR × T interaction, Table S4, Fig. S18).
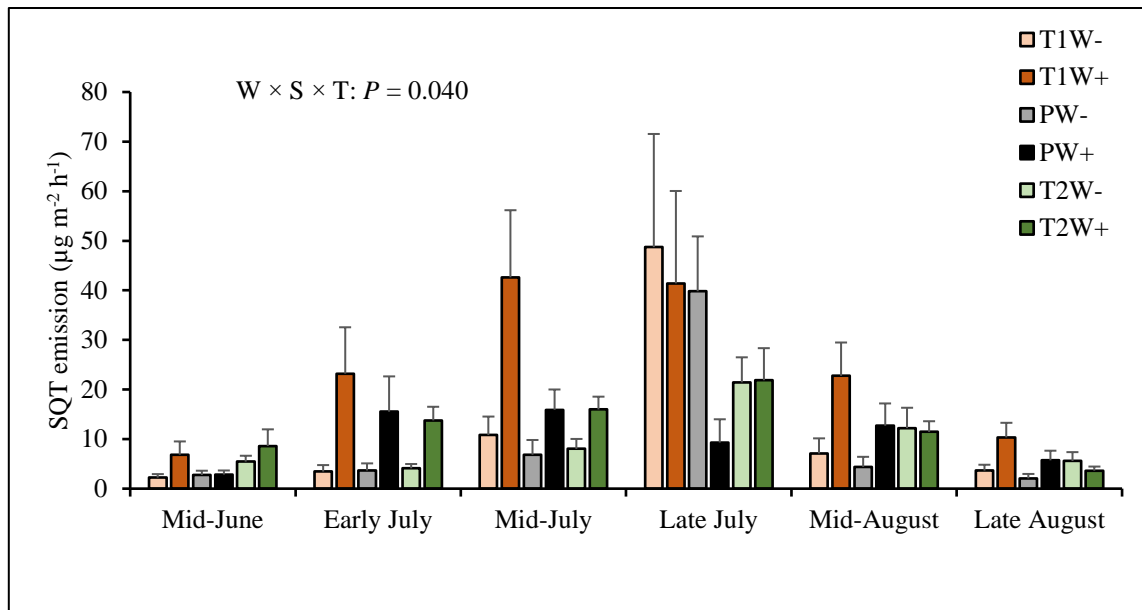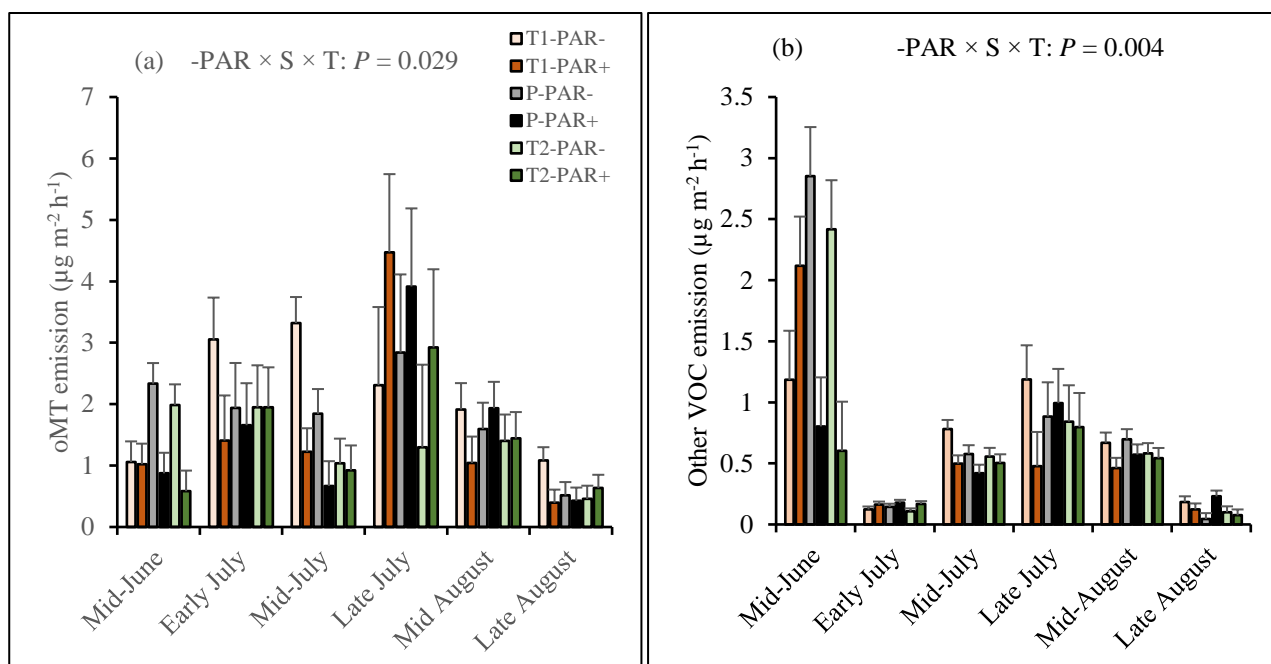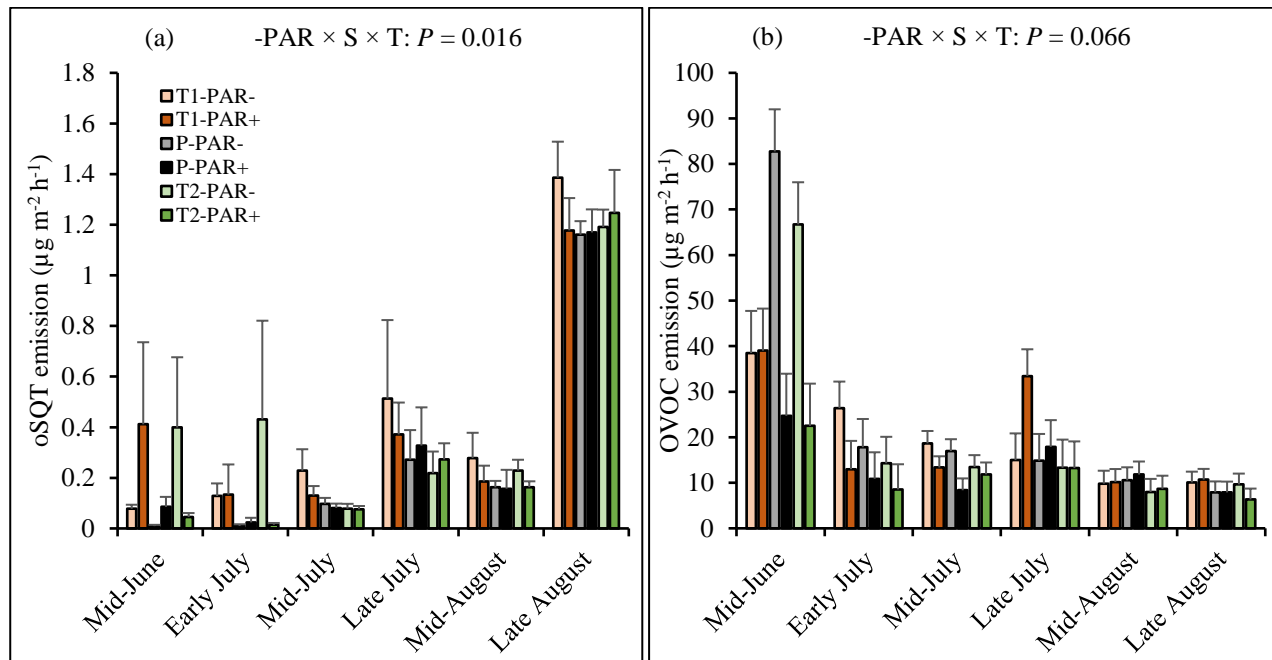
Fig. S9 SQT emissions from mesocosms from T1, P, and T2 sites under treatments with warming (W+, i.e., warming only and warming + increased cloudiness treatments) and without warming (W-, i.e., control and increased cloudiness only treatments) during the first growing season. Bars represent mean values per site per treatment (±SE, n = 10 per site per treatment) per measurement campaign. Abbreviations: T1 and T2 indicate the two locations within the tundra, P = palsa mire, T1W- = T1 site in treatments without warming, T1W+ = T1 site in treatments with warming, PW- = P site in treatments without warming, PW+ = P site in treatments with warming, T2W- = T2 site in treatments without warming, T2W+ = T2 site in treatments with warming, W × S × T = warming × site × time interaction. Statistically significant P-value < 0.05 from LMM ANOVA is shown. See table S3 for detailed statistics.
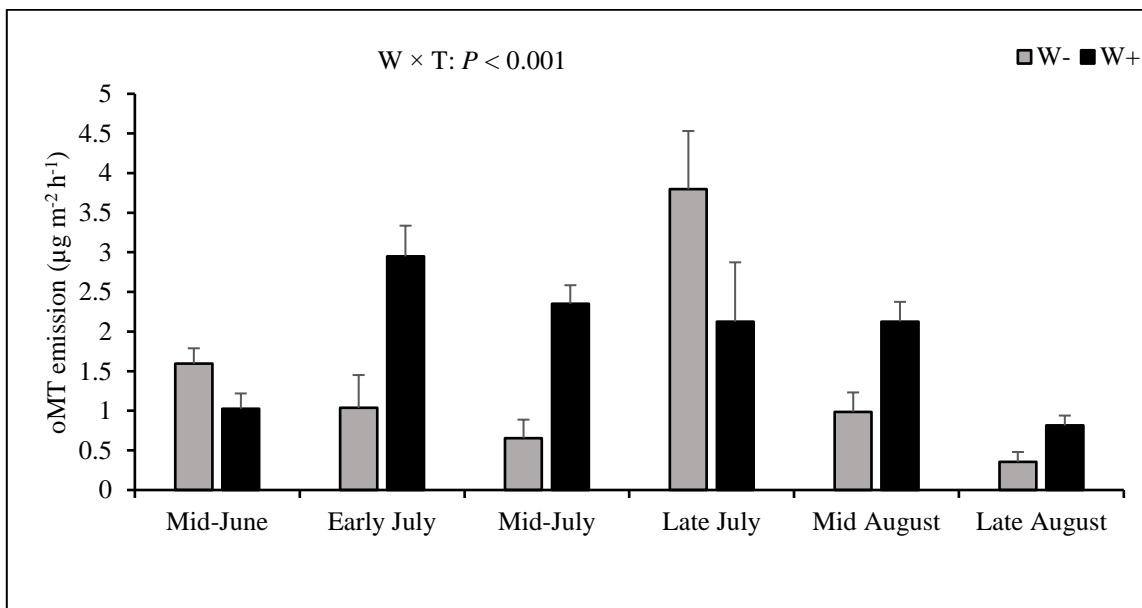
Fig. S10 oMT emissions across all sites under treatments with warming (W+, i.e., warming only and warming + increased cloudiness) and without warming (W-, i.e., control and increased cloudiness only) during the first growing season. Bars represent mean values per treatment (±SE, n = 30 per treatment) per measurement campaign. W × T = warming × time interaction. Statistically significant P-value < 0.05 from LMM ANOVA is shown. See table S3 for detailed statistics.

Fig. S11 (a) oMT and (b) Other VOC emissions from mesocosms from T1, P, and T2 sites under treatments with increased cloudiness (-PAR+, i.e., increased cloudiness only and warming + increased cloudiness treatments) and without increased cloudiness (-PAR-, i.e., control and warming only treatments) during the first growing season. Bars represent mean values per site per treatment (±SE, $n = 10$ per site per treatment) per measurement campaign. Abbreviations: T1 and T2 indicate the two locations within the tundra, P = palsa mire, T1-PAR- = T1 site in treatments without increased cloudiness, T1-PAR+ = T1 site in increased cloudiness treatments, P-PAR- = P site in treatments without increased cloudiness, P-PAR+ = P site in increased cloudiness treatments, T2-PAR- = T2 site in treatments without increased cloudiness, T2-PAR+ = T2 site in increased cloudiness treatments, -PAR × S × T = increased cloudiness × site × time interaction. Statistically significant *P*-values < 0.05 from LMM ANOVA are shown. See table S3 for detailed statistics.
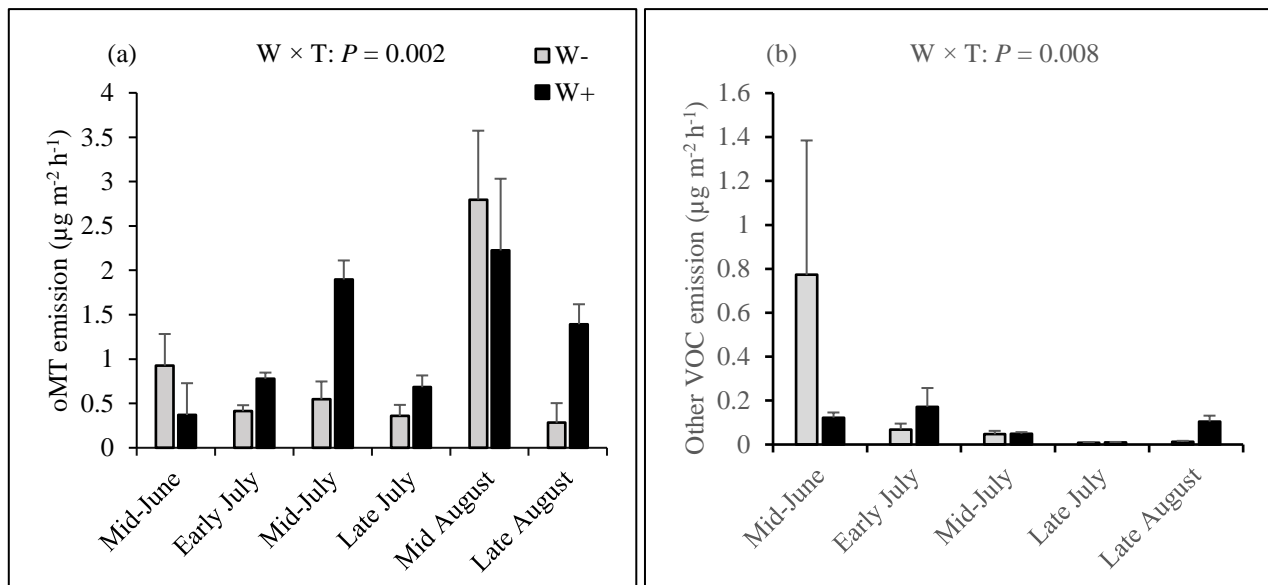

Fig. S12 (a) oSQT and (b) OVOC emissions from mesocosms from T1, P, and T2 sites under treatments with increased cloudiness (-PAR+, i.e., increased cloudiness only and warming + increased cloudiness treatments) and without increased cloudiness (-PAR-, i.e., control and warming only treatments) during the first growing season. Bars represent mean values per site per treatment (±SE, $n = 10$ per site per treatment) per measurement campaign. Abbreviations: T1 and T2 indicate the two locations within the tundra, P = palsa mire, T1-PAR- = T1 site in treatments without increased cloudiness, T1-PAR+ = T1 site in increased cloudiness treatments, P-PAR- = P site in treatments without increased cloudiness, P-PAR+ = P site in increased cloudiness treatments, T2-PAR- = T2 site in treatments without increased cloudiness, T2-PAR+ = T2 site in increased cloudiness treatments, -PAR × S × T = increased cloudiness × site × time interaction. Statistically significant *P*-values < 0.05 from LMM ANOVA are shown. See table S3 for detailed statistics.

Fig. S13 (a) OVOC (b) MT and (c) HC emissions from mesocosms across all sites in control (C), warming (W), increased cloudiness (-PAR), and warming + increased cloudiness (W-PAR) treatments during the first growing season. Bars represent mean values per treatment (±SE, n = 15 per treatment) per measurement campaign. W × -PAR × T = warming × increased cloudiness × time interaction. Statistically significant P-values < 0.05 from LMM ANOVA are shown. See table S3 for detailed statistics.
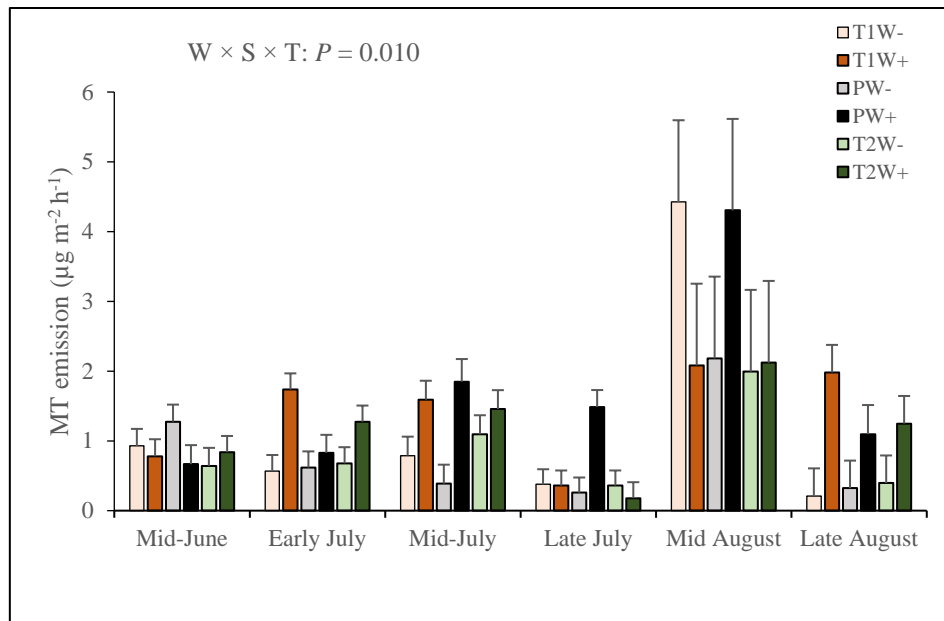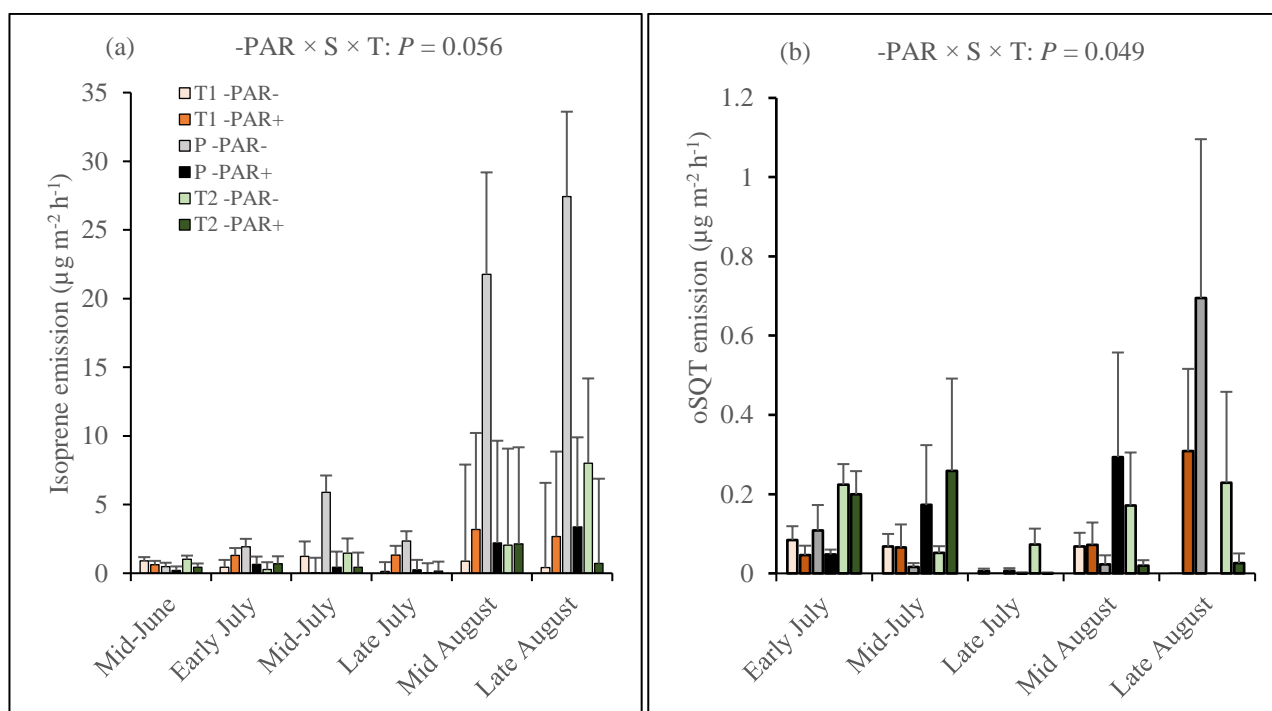
Fig. S14 MT emissions across all sites under treatments with warming (W+, i.e., warming only and warming + increased cloudiness treatments) and without warming (W-, i.e., control and increased cloudiness only treatments) during the second growing season. Bars represent mean values per site per treatment (±SE, n = 10 per site per treatment) for each measurement campaign. Abbreviations: T1 and T2 indicate the two locations within the tundra, P = palsa mire, T1W- = T1 site in treatments without warming, T1W+ = T1 site in warming treatments, PW- = P site in treatments without warming, PW+ = P site in warming treatments, T2W- = T2 site in treatments without warming, T2W+ = T2 site in warming treatments, W × S × T = warming × site × time interaction. Statistically significant P-value < 0.05 from LMM ANOVA is shown. See table S4 for detailed statistics.
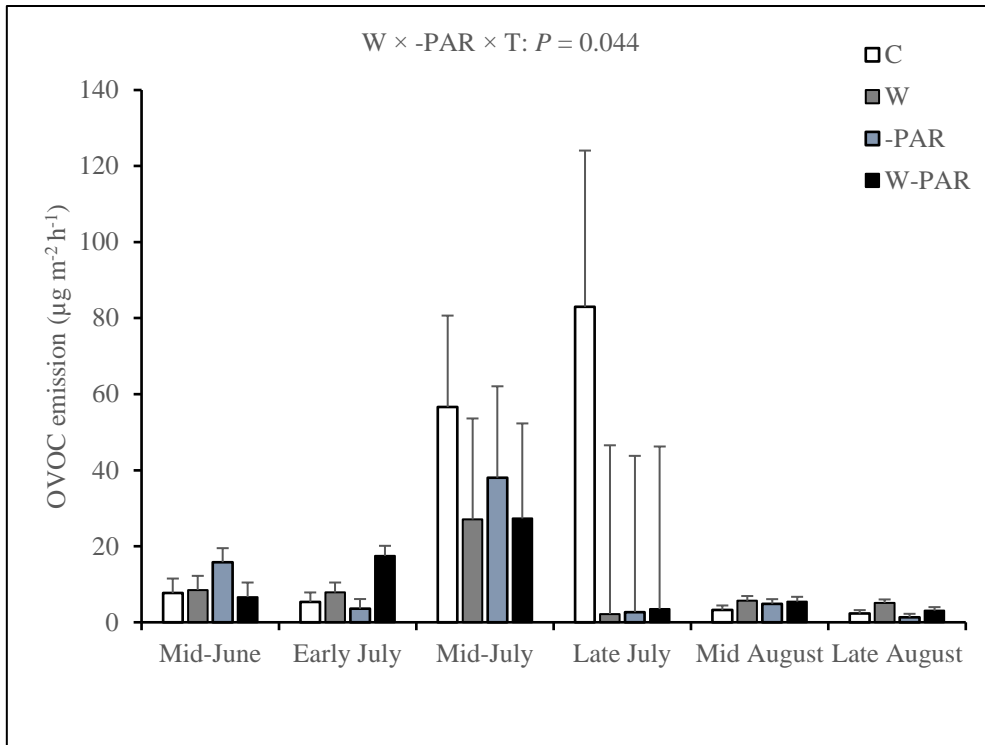

Fig. S15 (a) oMT and (b) other VOC emissions across all sites under treatments with warming (W+, i.e., warming only and warming + increased cloudiness) and without warming (W-, i.e., control and increased cloudiness only) during the second growing season. Bars represent mean values per treatment (±SE, n = 30 per treatment) per measurement campaign. W × T = warming × time interaction. Statistically significant P-values < 0.05 from LMM ANOVA are shown. See table S4 for detailed statistics.
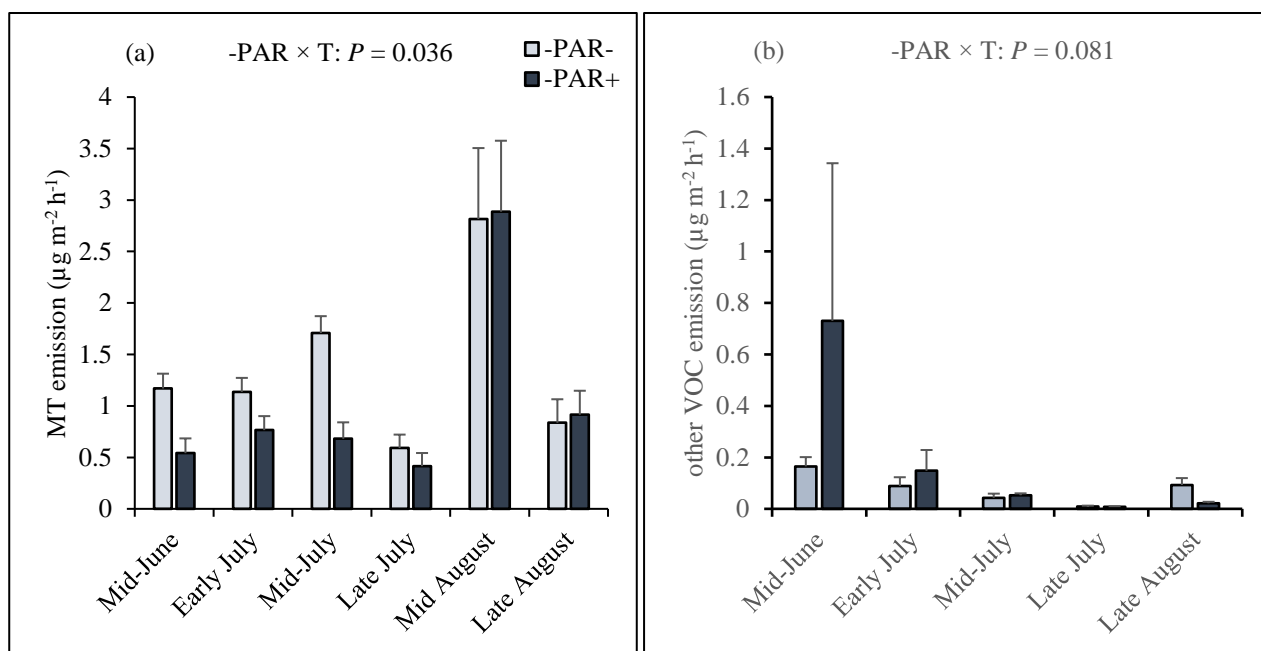
Fig. S16 (a) MT and (b) other VOC emissions across all sites under treatments with increased cloudiness (-PAR+, i.e., increased cloudiness only and warming + increased cloudiness treatments) and without increased cloudiness (-PAR-, i.e., control and warming only treatments) during the second growing season. Bars represent mean values per treatment (±SE, n = 30 per treatment) per measurement campaign. -PAR × T = increased cloudiness × time interaction. Statistically significant P-value < 0.05 and marginally significant P-value < 0.1 from LMM ANOVA are shown. See table S4 for detailed statistics.

Fig. S17 (a) Isoprene and (b) oSQT emissions from mesocosms from T1, P, and T2 sites under treatments with increased cloudiness (-PAR+, i.e., increased cloudiness only and warming + increased cloudiness treatments) and without increased cloudiness (-PAR-, i.e., control and warming only treatments) during the second growing season. Bars represent mean values per site per treatment (±SE, n = 10 per site per treatment) for each measurement campaign. Abbreviations: T1 and T2 indicate the two locations within the tundra, P = palsa mire, T1-PAR- = T1 site in treatments without increased cloudiness, T1-PAR+ = T1 site in increased cloudiness treatments, P-PAR- = P site in treatments without increased cloudiness, P-PAR+ = P site in increased cloudiness treatments, T2-PAR- = T2 site in treatments without increased cloudiness, T2-PAR+ = T2 site in increased cloudiness treatments, -PAR × S × T = increased cloudiness × site × time interaction. Statistically significant P-value < 0.05 and marginally significant P-value < 0.1 from LMM ANOVA are shown. See table S4 for detailed statistics.

Fig. S18 OVOC emissions from mesocosms across all sites in control (C), warming (W), increased cloudiness (-PAR), and warming + increased cloudiness (W-PAR) treatments during the second growing season. Bars represent mean values per treatment (±SE, $n = 15$ per treatment) per measurement campaign. W × -PAR × T = warming × increased cloudiness × time interaction. Statistically significant P-value < 0.05 from LMM ANOVA is shown. See table S4 for detailed statistics.
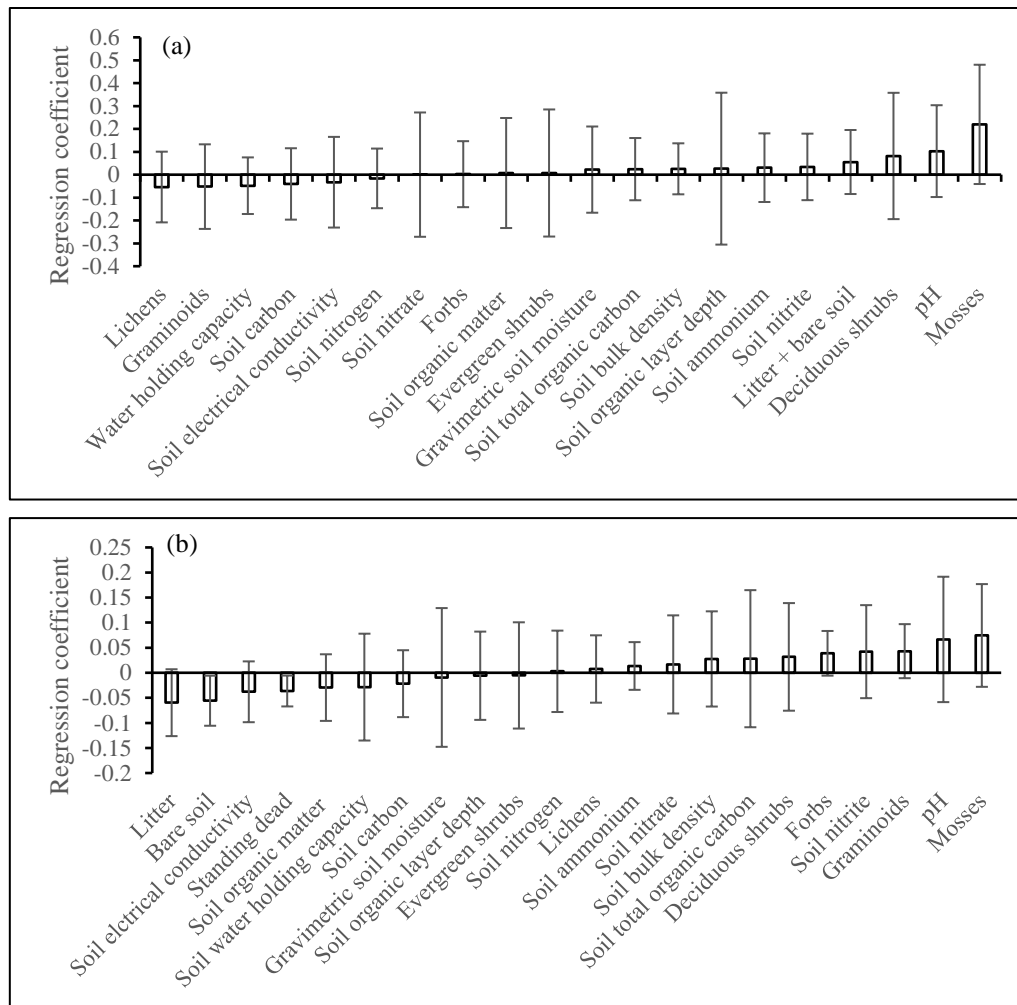
Fig. S19 Regression coefficients from PLS regression models on CH₄ flux during (a) the first and (b) second growing seasons. Error bars show ± 2 standard deviations of the regression coefficients.

References

1. H. R. Bhattarai, P. Virkajärvi, P. Yli-Pirilä and M. Maljanen, Emissions of atmospherically important nitrous acid (HONO) gas from northern grassland soil increases in the presence of nitrite (NO₂⁻), *Agr. Ecosyst. Environ.*, 2018, 256, 194–199, https://doi.org/10.1016/j.agee.2018.01.017.

2. K. Stemmler, M. Ammann, C. Donders, J. Kleffmann and C. George, Photosensitized reduction of nitrogen dioxide on humic acid as a source of nitrous acid, *Nature*, 2006, 440, 195-198, https://doi.org/10.1038/nature04603.

3. A. Stewart-Jones and G.M. Poppy, Comparison of Glass Vessels and Plastic Bags for Enclosing Living Plant Parts for Headspace Analysis. *J. Chem. Ecol.*, 2006, 32, 845–864, https://doi.org/10.1007/s10886-006-9039-6.

4. H. Valolahti, M. Kivimäenpää, P. Faubert, A. Michelsen and R. Rinnan, Climate change-induced vegetation change as a driver of increased subarctic biogenic volatile organic compound emissions, *Glob. Change Biol.*, 2015, 21, 3478-3488, https://doi.org/10.1111/gcb.12953.

5. B. Quintanilla Casas, R. Bro, J. Hinrich and C. Davie-Martin, Tutorial on PARADISe: PARAFAC2-based Deconvolution and Identification System for processing GC–MS data, 2023, https://doi.org/10.21203/rs.3.pex-2143/v1.